

Superconducting phase transition in quasi-two-dimensional Hubbard model

Xin-Zhong Yan

Institute of Physics, Chinese Academy of Sciences, P.O. Box603, Beijing 100080, China

E-mail: yanxz@aphy.iphy.ac.cn

(September 8, 2019)

The superconducting phase transition in quasi-two-dimensional Hubbard model is studied on the basis of spin and pairing fluctuations exchange approximation. The integral equations for the Green's function are self-consistently solved by numerical calculation. The superconducting-phase boundary obtained by the present calculation is compared with the experimental result for the cuprate high-temperature superconductors. Some numerical techniques are presented in details.

PACS numbers: 74.62.-c,74.20.-z,74.72.-h,74.40.+k

I. INTRODUCTION

The Hubbard model has been considered as the basic model to study the mechanism of high-temperature superconductivity in the cuprates.¹ By this model, the spin fluctuation exchange between electrons is considered as responsible for the mechanism of high-temperature superconductivity. A number of calculations, taking into account of the spin fluctuation effects, have been devoted to investigate the superconducting properties of the two-dimensional Hubbard models.^{2–12}

However, the pairing fluctuation is significant in the low-dimensional superconducting systems.^{13–16} According to the Mermin-Wagner-Hohenberg (MWH) theorem,¹⁷ there is no superconductivity at finite temperature in systems of dimension less than or equal to 2. The reason is that the pairing fluctuation is so strong that the condensation of electron pairs is prohibited. It is then natural to consider the quasi-two-dimensional (Q2D) Hubbard model for describing the electrons in the cuprate high-temperature superconductors. By using phenomenological Q2D models,^{15,16} it has been shown that the pairing fluctuations can result in considerable reduction of the transition temperature T_c . In addition, the pairing fluctuation is also relevant to the pseudogap phenomena^{15,16,18–21} observed in the normal state^{22,23} as well as in the superconducting state²⁴ of the cuprates.

In this work, we study the superconducting phase transition in the Q2D Hubbard model. In the present calculation, in addition to the spin fluctuations exchange (S-FLEX), we take into account of the contribution from the pairing fluctuation in the self-energy. The transition temperature so obtained by the present spin-pairing-fluctuations exchange (SP-FLEX) approximation is considerably reduced from that of S-FLEX approximation. The superconducting phase boundary by the present calculation is compared with the experimental results for the cuprate high-temperature superconductors. In the meanwhile, we also present some numerical techniques in details in the appendices, which is necessary for carrying out the numerical solution for the Green's function.

II. FORMALISM

The Q2D Hubbard model defined on a layered cubic lattice is of the following form²⁵

$$H = - \sum_{\langle \mathbf{ij} \rangle, \alpha} t_{\mathbf{ij}} c_{\mathbf{i}\alpha}^\dagger c_{\mathbf{j}\alpha} + U \sum_{\mathbf{i}} n_{\mathbf{i}\uparrow} n_{\mathbf{i}\downarrow} - \mu \sum_{\mathbf{i}} (n_{\mathbf{i}\uparrow} + n_{\mathbf{i}\downarrow}) \quad (1)$$

where $t_{\mathbf{ij}}$ denotes the hopping energy of electron between the lattice sites \mathbf{i} and \mathbf{j} , $c_{\mathbf{i}\alpha}^\dagger$ ($c_{\mathbf{i}\alpha}$) represents the electron creation (annihilation) operator of spin- α at site \mathbf{i} , $n_{\mathbf{i}\alpha} = c_{\mathbf{i}\alpha}^\dagger c_{\mathbf{i}\alpha}$, U is the on-site Coulomb interaction, and μ is the chemical potential. The $\langle \mathbf{ij} \rangle$ sum runs over the nearest-neighbor (NN) sites. In the following, we shall assume that $t_{\mathbf{ij}} = t$ for the intra-layer NN hopping and $t_{\mathbf{ij}} = t_z$ for the interlayer NN hopping. A quasi-two-dimensional system is characterized by the condition $t_z/t \ll 1$. Throughout this paper, we use unites in which $\hbar = k_B = 1$.

For simplifying the Feynman diagrams for the Green's function, we here present the approximation scheme for the normal state. This is enough for studying superconducting phase transition under consideration. The result for the superconducting state can be immediately obtained by adding the anomaly Green's function contributions. The Green's function for the electrons is given by

$$G(\mathbf{k}, z_n) = \frac{1}{z_n - \xi_{\mathbf{k}} - \Sigma(\mathbf{k}, z_n)} \quad (2)$$

where $z_n = i(2n - 1)\pi T$ with T the temperature of the system is the imaginary fermionic Matsubara frequency, $\xi_{\mathbf{k}} = -2t(\cos k_x + \cos k_y) - 2t_z \cos k_z - \mu$, and $\Sigma(\mathbf{k}, z_n)$ stands for the electron self-energy. For brevity, occasionally, we use the generalized momentum $k = (\mathbf{k}, z_n)$ in this paper. Figure 1 shows the approximation scheme for the self-energy. The first two diagrams in Fig. 1(a) are the well-known S-FLEX approximation. These two diagrams can be combined into a single diagram by redefining an

effective interaction V_{eff} that is the summation of two interactions given by Figs. 1(b) and 1(c). The expression for V_{eff} is

$$V_{\text{eff}}(q) = \frac{3}{2} \frac{U^2 \chi(q)}{1 + U \chi(q)} + \frac{1}{2} \frac{U^2 \chi(q)}{1 - U \chi(q)} - U^2 \chi(q) \quad (3)$$

with

$$\chi(q) = \frac{T}{N} \sum_k G(k+q)G(k). \quad (4)$$

The generalized momentum q stands for (\mathbf{q}, Z_m) with $Z_m = i2m\pi T$ the bosonic Matsubara frequency. The first and second terms in right-hand-side of Eq. (3) come respectively from the spin and charge fluctuations. The last term eliminates a double counting in the second-order diagrams. Owing to the spin fluctuation is predominant, it is named as spin fluctuation exchange approximation. The Hartree term has been neglected since it is a constant, which can be absorbed in the chemical potential. In the present calculation, we add the third diagram in Fig. 1(a) representing the contribution from the pairing fluctuation. Apart from two interaction sides, the shaded part essentially represents the processes of the electron pair propagating. Fig. 1(d) gives the ladder-diagram approximation for it with the second order term given by Fig. 1(e) and two pairing interactions respectively given Figs. 1(c) and 1(f). For brevity, we have dropped all the momentum on these diagrams. The momentum and spins attached to the ladder-diagram are illustrated in Fig. 2. For the sake of discussion, we here introduce a notation $L_{\alpha\beta, \beta'\alpha'}(k, q-k; q-k', k')$ for the ladder-diagram.

To see how the pairing fluctuation takes effect, we consider Fig. 1(d) for the case of a pair of electrons with opposite spin and opposite momentum. Because of $L_{\alpha\beta, \beta'\alpha'}(k, -k; -k', k') = -L_{\beta\alpha, \alpha'\beta'}(-k, k; -k', k')$, we thereby can combine the last two terms in Fig. 1(d) with an effective pairing interaction V_P defined by Fig. 3(b), and obtain an equation like to Fig. 3(c) but with ‘ \approx ’ replaced by ‘=’ under the ladder-diagram approximation. To solve this equation, we expand the effective pairing interaction in terms of a complete set of basis functions ϕ_n ,

$$V_P(k, k') = \sum_n v_n \phi_n(k) \phi_n(k'). \quad (5)$$

The function ϕ_n satisfies the eigen equation [see Fig. 3(c)]

$$\frac{T}{N} \sum_{k'} V_P(k, k') G(k') G(-k') \phi_n(k') = \lambda_n \phi_n(k) \quad (6)$$

where N is the total number of lattice sites, and λ_n is the eigenvalue. By so doing, we get

$$L_{\alpha\beta, \beta'\alpha'}(k, -k; -k', k') = - \sum_n \frac{\lambda_n v_n \phi_n(k) \phi_n(k')}{1 - \lambda_n}. \quad (7)$$

In the superconducting state, the largest eigenvalue equals to unity, by which the eigen equation (6) then reduces to the gap equation. Therefore, $L_{\alpha\beta, \beta'\alpha'}(k, -k; -k', k')$ is singular. It implies that the long-wave pairing fluctuation gives significant contribution to the self-energy. On the other hand, as $T \rightarrow T_c$ from the normal state, with the largest eigen value of Eq. (6) approaching to unity, $L_{\alpha\beta, \beta'\alpha'}(k, -k; -k', k')$ diverges at this limit. Therefore, at T close to T_c , we can consider only the pairing of largest eigenvalue. For the present case, the largest one is the d -wave pairing. Hereafter, we denote the largest eigenvalue and the corresponding eigen function simply as λ_d and $\phi(k)$, respectively, and the coupling constant simply by v .

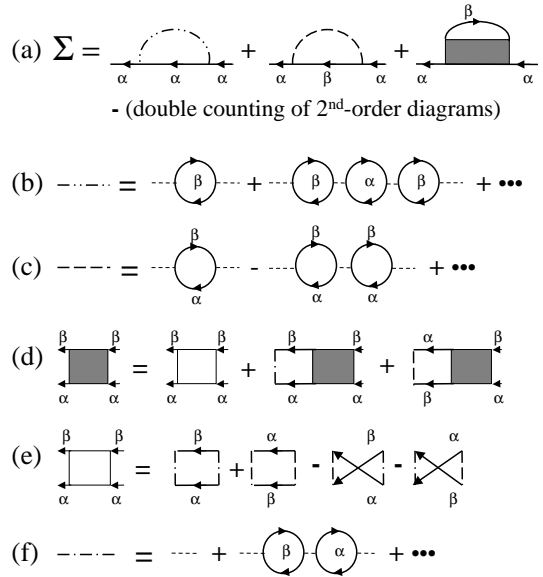


FIG. 1. Approximation scheme for the self-energy. (a) Self-energy for the α -spin electrons. The first term comes from the coupling of the α -spin electrons with the density fluctuation of opposite β -spin electrons. The second term is due to the interaction between transverse spins and their fluctuation. The last term represents the contribution from the pairing fluctuation. (b) Interaction between α -spin electrons due to the density fluctuation of β -spin electrons. (c) Interaction between transverse spins stemming from their fluctuation. (d) Ladder-diagram approximation to the pairing fluctuation. (e) Second order ladder-diagrams. (f) Effective interaction between electrons of opposite spins.

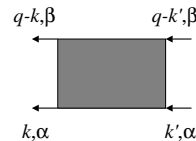


FIG. 2. Ladder-diagram representing the propagating of a pair of total momentum q . k' and $q-k'$ are the initial momentum of the α and β -spin electrons, respectively. After propagating, their momentum change to k and $q-k$.

On observing the above-mentioned fact, we make the

approximation in Fig. 1(d) using the pairing interactions of zero total momentum because the long-wave pairing fluctuation gives the predominant contribution. We then obtain equations as given by Fig. 3 for determining $L_{\alpha\beta,\beta'\alpha'}(k, q-k; q-k', k')$. Furthermore, by considering only the d -wave pairing, the ladder diagram summation can be factorized as

$$L_{\alpha\beta,\beta'\alpha'}(k, q-k; q-k', k') = P(q)\phi(k)\phi(k'), \quad (8)$$

with

$$P(q) = \frac{v^2\Pi(q)}{1+v\Pi(q)} - v^2\Pi(q) \quad (9)$$

$$\Pi(q) = -\frac{T}{N} \sum_k \phi^2(k)G(k)G(q-k). \quad (10)$$

In Eq. (9), the last term eliminates all the second-order diagrams since the contribution to the self-energy from the first two diagrams in the right-hand side of the diagrammatic equation of Fig. 1(e) has been taken into account in S-FLEX approximation, while the other two are negligible with comparing to the infinitive ladder-diagram summation. For the self-energy, the final expression is

$$\Sigma(k) = -\frac{T}{N} \sum_q G(k-q)V_{\text{eff}}(q) + \frac{T\phi^2(k)}{N} \sum_q G(q-k)P(q). \quad (11)$$

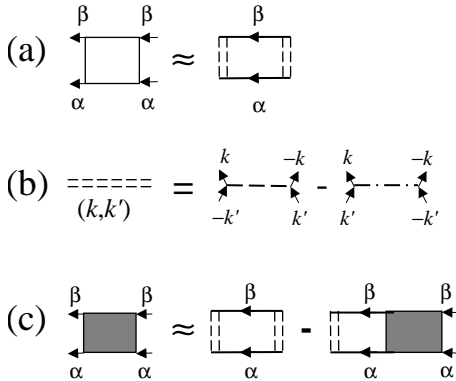


FIG. 3. Approximation to the ladder-diagram. (a) Approximate second order ladder-diagram obtained from Fig. 1(e) by neglecting the dependence of the interactions on the total momentum of the pair. (b) Effective pairing interaction. (c) Renormalized diagrammatic equation for the ladder-diagram.

For the Q2D system, $t_z/t \ll 1$, the Green's function $G(k)$ has a very weak dependence on k_z . Similarly, $\chi(q)$ and $\Pi(q)$ very weakly depends on q_z . However, the function $P(q)$ has a delicate dependence on q_z . Consider the case at small q . Since $\Pi(q)$ is an even function of q , at small \mathbf{q} and $Z_m = 0$, we have

$$1 + v\Pi(\mathbf{q}, 0) \approx d + c(q_x^2 + q_y^2) + c_z q_z^2 \quad (12)$$

where d , c and c_z are constants. The q_z^2 -term in Eq. (12) comes from the interlayer electron hopping. The ratio c_z/c is much less than unity. At $T \rightarrow T_c$, d vanishes at this limit since $P(q)$ diverges, as shown above, at $q = 0$. If the q_z dependence in $P(q)$ is ignored, the second summation in the right-hand side of Eq. (11) will be divergent at $T_c \neq 0$, which implies there will be no superconductivity in the system at finite temperature. This conclusion is consistent with the MWH theorem.¹⁷ We therefore keep the q_z -dependence in the denominator of $P(q)$ to the order of q_z^2

$$1 + v\Pi(q) = 1 + v\bar{\Pi}(q) + c_z q_z^2 \quad (13)$$

with

$$\bar{\Pi}(q) = \Pi(q)|_{q_z=0} \quad (14)$$

$$c_z = \frac{v}{2} \frac{d^2}{dq_z^2} \Pi(q)|_{q=0} \quad (15)$$

and use $\bar{\Pi}(q)$ for $\Pi(q)$ in the nominator in Eq. (9). By neglecting the q_z -dependence in the Green's function, the second summation over q_z in Eq. (11) can be taken immediately. Therefore, instead of $P(q)$ in Eq. (11) we insert in a function defined by

$$P_{\text{eff}}(q) = \frac{1}{\pi} \int_0^\pi dq_z P(q) \quad (16)$$

$$= -\frac{v^3 \bar{\Pi}^2(q)}{\pi c_z} \gamma(q) \text{atan}[\pi \gamma(q)], \quad (17)$$

with

$$\gamma(q) = \left[\frac{c_z}{1 + v\bar{\Pi}(q)} \right]^{1/2}.$$

To evaluate the constant c_z , we need to take the derivative of the Green's function $G(q-k)$ with respect to q_z as indicated by Eqs. (10) and (15). By neglecting the q_z -dependence of the self-energy, $G(q-k)$ thereby depends on q_z only via ξ_{q-k} . It is expectable that such an approximation does not change the physical result so much. To the second order of t_z/t , we obtain¹⁶

$$c_z = \frac{t_z^2 v T}{N} \sum_k \phi^2(k) \left| \frac{\partial}{\partial \xi_k} G(k) \right|^2, \quad (18)$$

with

$$\frac{\partial}{\partial \xi_k} G(k) \approx G^2(k). \quad (19)$$

In addition, the chemical potential μ should be determined to yield the hole concentration

$$\delta = -\frac{T}{N} \sum_k [G(k) + G(-k)]. \quad (20)$$

So far, the above equations form the closed system that self-consistently determines the Green's function.

III. NUMERICAL RESULTS

Since the functions $G(k)$, $V_{\text{eff}}(q)$ and $P_{\text{eff}}(q)$ are defined in multi-dimensional space, they require huge memory storage in the numerical computation process. Especially, the function $P_{\text{eff}}(q)$ is singular at $q = 0$ and $T \leq T_c$. Therefore, to carry out the numerical solution, we need to develop numerical schemes to reduce the amount of computation without losing the accuracy. In Appendix A, we present our scheme for the Matsubara frequency summation. The summation is taken over 57 points, a subset of the frequencies, in a sufficiently large range. The cutoff frequencies are $z_c = (2N_c - 1)\pi T$ for the fermions and $Z_c = 2(N_c - 1)\pi T$ for the bosons, respectively, with $N_c = 1017$. For the typical temperature $T/t \sim 0.007$ under consideration, this means $2N_c\pi T/t \sim 45$. For calculating the function $\chi(q)$, beyond this range, the summation over the terms of $n > N_c$ is analytically carried out by using the asymptotic formula of the Green's function

$$G(\mathbf{k}, z_n) \rightarrow 1/z_n. \quad (21)$$

The error of the summation over the terms of $n > N_c$ is of the order $O(z_c^{-3})$.

The convolutions in the momentum space are carried out with fast Fourier transforms (FFTs) on a 128×128 lattice. For inverse transform of $V_{\text{eff}}(\mathbf{q}, 0)$ and $P_{\text{eff}}(\mathbf{q}, 0)$, i.e., from momentum space to real space, we have to pay special care. At low temperature, $V_{\text{eff}}(\mathbf{q}, 0)$ has strong peaks near $\mathbf{q} = (\pi, \pi)$.⁷ We therefore use a 256×256 mesh in momentum space for the inverse transform. The values of $V_{\text{eff}}(\mathbf{q}, 0)$ for this mesh are obtained by local quadratic polynomial interpolation of the smooth function $\chi(q)$ given on a 128×128 mesh. On the other hand, the function $P_{\text{eff}}(\mathbf{q}, 0)$ has divergently sharp peak at $\mathbf{q} = 0$ at $T = T_c$. In Appendix B, we deal with the inverse transform of this function.

It is impossible to solve Eq. (6) in momentum space because the memory requirement for the coefficient matrix is prohibitive. In Appendix C, we rewrite the eigen equation in real space. This reduces greatly the amount of numerical calculation work.

In the present calculation, we set $U/t = 6$ and $t_z/t = 0.01$. In Fig. 4, we show the result for the eigenvalue λ_d as function of T at $\delta = 0.125$. The S-FLEX result is also presented for comparison. Due to the pairing fluctuation, the eigenvalue by the present SP-FLEX approximation is reduced from that of the S-FLEX, giving rise to a lower transition temperature, $T_c/t = 0.0056$. The S-FLEX result is $T_c/t = 0.0266$. When using a further approximation $\phi(\mathbf{k}, z_n) = \Delta(z_n)(\cos k_x - \cos k_y)$, we get $T_c/t = 0.0275$ by the S-FLEX approximation, which is consistent with the existing results.⁷ By the S-FLEX approximation, we have $d\lambda_d(T)/dT \neq 0$ at $T = T_c$. It means that at $T < T_c$, by keeping no superconductive pairing, the S-FLEX approximation allows a solution of

$\lambda_d > 1$. In contrast to this feature of the S-FLEX approximation, the present solution for λ_d can never get across the line $\lambda_d = 1$. At $T \rightarrow T_c$, the pairing fluctuation effect is more pronouncedly with $\lambda_d \rightarrow 1$, which conversely suppresses λ_d . As a result, λ_d approaches to the unity slowly as $T \rightarrow T_c$. Therefore, the curve $\lambda_d(T)$ is tangent to the straight line $\lambda_d = 1$ at T_c , i.e.,

$$\frac{d}{dT}\lambda_d(T)|_{T_c} = 0. \quad (22)$$

The inset of Fig. 4 shows that $\sqrt{1 - \lambda_d}$ varies nearly linearly as $T \rightarrow T_c$, which means $1 - \lambda_d \propto (T - T_c)^2$.

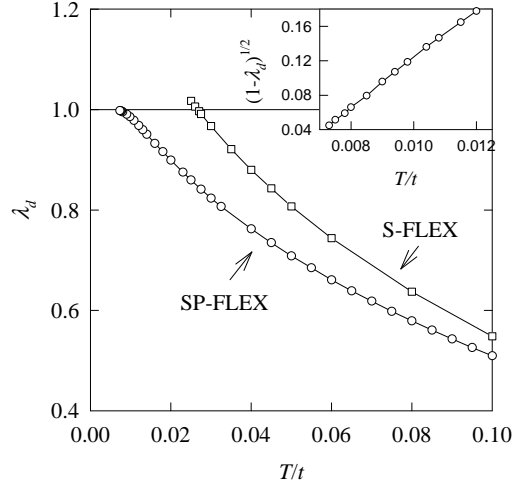


FIG. 4. Eigen value λ_d as function of T at $\delta = 0.125$. SP-FLEX is the present calculation. The result of S-FLEX is also depicted for comparison. The inset shows $(1 - \lambda_d)^{1/2}$ of the present calculation as function of T .

Shown in Fig. 5 are the results for λ_d as functions of T at various δ . Close to $\lambda_d = 1$, all the curves have the same feature as shown in Fig. 4; each curve is smoothly connected to the straight line $\lambda_d = 1$. The transition temperature T_c is determined by $\lambda(T_c) = 1$. The boundary of superconducting phase in the $T_c - \delta$ phase diagram is depicted in Fig. 6. For comparison, we also show the results of the S-FLEX approximation and the experiments²⁶ for the cuprate high-temperature superconductors. Due to the pairing fluctuation, T_c is considerably reduced from that by the S-FLEX approximation. The reduction is more significant at lower hole doping where the transition temperature decreases with decreasing δ . This qualitatively reflects the feature of the experimental results. On the other hand, at large δ , the pairing fluctuation is less pronouncedly. This is consistent with the previous conclusion.¹⁶

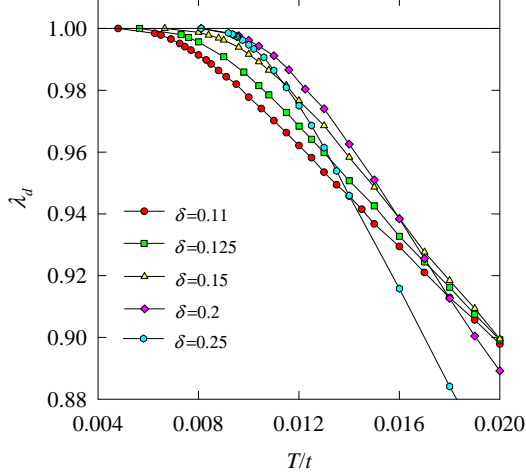


FIG. 5. Eigen value λ_d as function of T at varies δ .

To see why the pairing fluctuation results in reduction of T_c , we analyze the self-energy given by Eq. (11) with $P(q)$ replaced by $P_{\text{eff}}(q)$. At $Z_m \simeq 0$, since $V_{\text{eff}}(q)$ and $P_{\text{eff}}(q)$ have strong negative peaks respectively at $\mathbf{q} = \mathbf{Q} \equiv (\pi, \pi)$ and $\mathbf{q} = 0$, we here make a crude approximation (for the sake of illustration) for the self-energy,

$$\begin{aligned} \Sigma(k) \approx & -G(\mathbf{k} - \mathbf{Q}, z_n) \left[\frac{T}{N} \sum_{q \sim \mathbf{Q}} V_{\text{eff}}(q) \right] \\ & + G(\mathbf{k}, -z_n) \left[\frac{T \phi^2(k)}{N} \sum_{q \sim 0} P_{\text{eff}}(q) \right]. \end{aligned} \quad (23)$$

The summations in the square brackets give rise to two negative quantities. At small δ , $\mu \approx 0$, we have $G(\mathbf{k} - \mathbf{Q}, z_n) \approx -G(\mathbf{k}, -z_n)$. Taking into account of these facts, we get $\Sigma(k) \approx -G(\mathbf{k}, -z_n) \Gamma_k^2$ with $\Gamma_k^2 = a_1 + a_2 \phi^2(k)$, where a_1 and a_2 are two positive constants. Substituting the result into Eq. (2), one obtains

$$G(\mathbf{k}, z_n) \approx \frac{z_n + \xi_k}{2\Gamma_k^2} \left(1 - \sqrt{1 + \frac{4\Gamma_k^2}{\xi_k^2 - z_n^2}} \right). \quad (24)$$

Applying these results to Eq. (6), we see that the factor $G(k)G(-k)$ is reduced, and so is T_c .

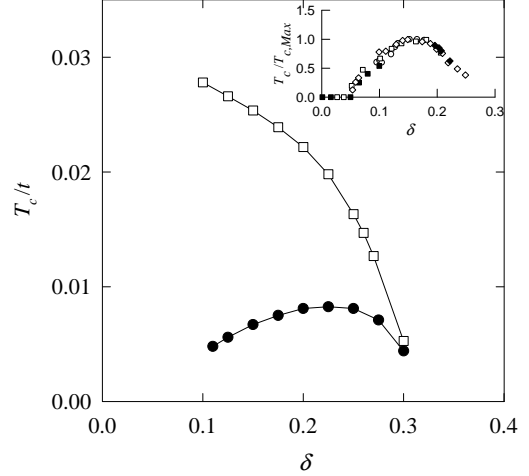


FIG. 6. Transition temperature T_c as function of hole concentration δ . The solid circles are obtained by the present calculation. The squares representing the results of the S-FLEX approximation are presented for comparison. The inset shows the experimental results for the cuprate high-temperature superconductors.

Physically, the quantity

$$a_2 = -\frac{T}{N} \sum_{q \sim 0} P_{\text{eff}}(q)$$

is a measure of the density of pairs at their excited states. Since the function $P_{\text{eff}}(q)$ is given in terms of $\bar{\Pi}(q)$ by (17), we analyze $\bar{\Pi}(q) = \Pi(q)|_{q_z=0}$ especially at $q = 0$. From Eq. (10), we see that the quantity $\Pi(0)$ comes predominately from the summation over the points close to the Fermi surface in momentum space. At smaller δ , the Fermi surface of the Hubbard model is larger, so is the number of the pairs at their fluctuating states. Therefore, the reduction on T_c is larger at smaller δ .

The form of the Green's function given by Eq. (24) implies that there exists a pseudogap in the energy spectrum of the electrons.^{16,27} Consider the spectral function

$$\begin{aligned} A(\mathbf{k}, E) &= -\frac{1}{\pi} \text{Im} G(\mathbf{k}, E + i0^+) \\ &= \frac{E + \xi_k}{2\pi \Gamma_k^2} \sqrt{\frac{\xi_k^2 + 4\Gamma_k^2 - E^2}{E^2 - \xi_k^2}}, \end{aligned}$$

which is nonzero only for $E^2 - 4\Gamma_k^2 < \xi_k^2 < E^2$. The noninteraction delta-function peak becomes a square root singularity. Because of the constraint, the area of the \mathbf{k} -space of $A(\mathbf{k}, E) \neq 0$ decreases at $E \rightarrow 0$, resulting in a suppression of the density of states. Especially, the density of states vanishes at $E = 0$ since the area becomes to zero and the singularity disappears there.

On observing the function Γ_k^2 , we note that the pseudogap stems from the spin and pairing fluctuations. Even at $T = 0$, the superconducting state can remain the pseudogap because the spin fluctuation (owing to which the

superconductivity takes place) and the pairing fluctuation (coming from the Goldstone mode¹⁶) exist. This may explain the recent experiment by Tallon *et al.*²⁴

IV. CONCLUSION

In summary, we have investigated the d -wave superconducting phase transition in the quasi-two-dimensional Hubbard model. The pairing fluctuation as well as the spin fluctuation is taken into account in the self-energy. By self-consistently solving the integral equations for the Green's function, we have obtained the transition temperature as function of hole concentration. The boundary of superconducting phase by the present calculation can reasonably reflect the feature of the experimental results for the cuprate high-temperature superconductors at small hole doping.

The pairing fluctuation implies that an amount of pairs occupy their excited states. This fluctuation effect leads to the reduction of the condensation of the pairs and thereby the transition temperature. On the other hand, the spin fluctuation produces the attraction between the electrons, resulting in the superconducting phase transition. In the meanwhile, the spin and pairing fluctuations commonly bring about a pseudogap to the electrons.

ACKNOWLEDGMENTS

The author thanks Prof. C. S. Ting for useful discussions on the related problems. This work was supported by Natural Science Foundation of China under grant number 10174092 and by Department of Science and Technology of China under grant number G1999064509.

APPENDIX A

In this appendix, we intend to develop an algorithm for the approximate summation of a series. It is analogous to Simpson's integral method. Firstly, we consider the following summation,

$$S(n_0, n_2) = \sum_{n=n_0}^{n_2} f(n), \quad (A1)$$

where $n_2 = n_0 + 2h$ with h an integer. Suppose $f(x)$ is a smooth function over the range $n_0 < x < n_2$. We then expand $f(n)$ as

$$f(n) \approx f(n_0) + c_1(n - n_0) + c_2(n - n_0)^2 \quad (A2)$$

where c_1 and c_2 are constants. With the given values $f_j \equiv f(n_0 + jh)$, for $j = 0, 1$ and 2 , the constants can be expressed as

$$c_1 = (-3f_0 + 4f_1 - f_2)/2h$$

$$c_2 = (f_0 - 2f_1 + f_2)/2h^2.$$

Substituting Eq. (A2) into Eq. (A1), we get

$$S(n_0, n_2) \approx \frac{h}{6}(2 + 3y + y^2)(f_0 + f_2) + \frac{h}{3}(4 - y^2)f_1, \quad (A3)$$

with $y = 1/h$. Therefore, the summation over the entire range $[n_0, n_2]$ can be obtained approximately with only three values f_0, f_1 and f_2 given. At $y \rightarrow 0$, Eq. (A3) reduces to the Simpson rule. With the approximation (A2), we even can carry out a summation over a part of the range $[n_0, n_2]$. For more general uses, for $n_0 \leq m \leq n_2$, we have

$$S(n_0, m) \approx Af_0 + Bf_1 + Cf_2 \quad (A4)$$

with

$$A = h(y + z)[1 - 3z/4 + z(y + 2z)/12]$$

$$B = h(y + z)z[1 - (y + 2z)/6]$$

$$C = -h(y + z)z[1 - (y + 2z)/3]/4$$

and $z = (m - n_0)/h$.

Now, we consider the summation $S(1, \infty)$. When $f(n)$ decreases fast at $n \rightarrow \infty$, $S(1, \infty)$ can be obtained approximately over a finite range with the cutoff number sufficiently large. We may divide this range into several blocks within each of which $f(x)$ can be regarded as smooth function and thereby the above algorithm can be applied. At most cases, $f(n)$ may vary fast at small n . Therefore, the stride h should be shorter at smaller n . Here, we introduce a point-selection program. Consider L successively connected blocks. The selected points divide each block into $M - 1 (\geq 2)$ equal-spaced segments; each block contains M points. The stride (the length of the segment) in the l -th block is $h_l = h^{l-1}$ with h a constant integer number. By such a program, the number of the j -th point in the l -th block is

$$n_{[j,l]} = (j - 1 + \frac{M - 1}{h - 1})h^{l-1} - \frac{M - h}{h - 1}, \quad (A5)$$

for $j = 1, 2, \dots, M$ and $l = 1, 2, \dots, L$. The cutoff number is $N_c = n_{[M,L]}$. By repeatedly using the above summation scheme, one can get approximately

$$S(1, \infty) \approx \sum_p w_p f(n_p), \quad (A6)$$

where p runs over the $L(M - 1) + 1$ selected points, and w_p is the weight at point $p \equiv [j, l]$; note that because of $n_{[M,l]} = n_{[1,l+1]}$, such of these points should be counted once in the summation. The point-selection program uniquely determines the weights. If $M \geq 5$ is an odd number, applying the above summation scheme, we can get

$$w_{[1,1]} = 1$$

$$w_{[j,l]} = (4h^{l-1} - h^{1-l})/3, \quad \text{for } j = 2, 4, \dots, M-1$$

$$w_{[j,l]} = (2h^{l-1} + h^{1-l})/3, \quad \text{for } j = 3, 5, \dots, M-2$$

$$w_{[M,1]} = (2h + 3 + h^{-1})/6$$

$$w_{[M,l]} = w_{[l+1,1]} = h^l(1 + h^{-1})/3 + (1 + h)h^{-l}/6,$$

$$\text{for } l = 2, \dots, L-1$$

$$w_{[M,L]} = h^{L-1}/3 + 1/2 + h^{1-L}/6.$$

To justify the above summation scheme, we here give an example. Consider the summation

$$S = \sum_{j=1}^{\infty} \frac{2}{4j^2 - 1} = 1. \quad (\text{A7})$$

Applying the above scheme with $h=2$, $L=7$, and $M=9$, we have

$$Sum = \sum_p \frac{2w_p}{4n_p^2 - 1} = 0.99952. \quad (\text{A8})$$

The relative error is $(Sum - S)/S = -4.8 \times 10^{-4}$. Note that the terms under the summation in Eq. (A7) decreases as $1/2j^2$ at large j . If one uses the known result

$$\sum_{j=1}^{\infty} j^{-2} = \pi^2/6,$$

the accuracy of the summation can be improved much better. Instead of Eq. (A8), we calculate the following summation

$$Sum = \sum_p w_p \left(\frac{2}{4n_p^2 - 1} - \frac{1}{2n_p^2} \right) + \pi^2/12. \quad (\text{A9})$$

With such an arrangement, the terms under the p -summation decreases as $O(n_p^{-4})$ at large n_p . This summation gives a very accurate result $Sum = 1.00000015$, with a small relative error 1.5×10^{-7} only.

In some cases, with the given points $n_{[j,l]}$ selected in advance, we need to calculate the summations, $S(1, n)$, with $n_{[j_0, l_c]} \leq n < n_{[j_0+1, l_c]}$ and $l_c \leq L$. In these cases, because the summation over a range needs three points at least, the terminate number $n_c \equiv n_{[j_c, l_c]}$ is then determined as follows

$$j_c = \begin{cases} 3, & \text{if } j_0 = 1 \\ j_0 + 1, & \text{otherwise.} \end{cases}$$

Since the summation $S(1, n)$ can be expressed as $S(1, n) = S(1, n_{[1, l_c]} - 1) + S(n_{[1, l_c]}, n)$, the weights at the points $n_p < n_{[1, l_c]}$ as tabulated above is unchanged,

while at the points $n_{[j, l_c]}$, for $j = 1, \dots, j_c$, w_p should be reevaluated according to the scheme as given by Eq. (A4)

For testing the accuracy of the scheme for summations of finite terms, we consider the following example

$$S_n = \sum_{j=1}^n \frac{2}{4j^2 - 1} = \frac{2n}{2n+1}. \quad (\text{A10})$$

With the $[h, L, M] = [2, 7, 9]$ program, the summation is approximated as

$$Sum = \sum_p \frac{2w_p^n}{4n_p^2 - 1} \quad (\text{A11})$$

where we use the superscript n indicating the n -dependence of the weights. The results for Sum/S_n are given in Table I. The relative error $R.E. = (Sum - S_n)/S_n$ is less than 10^{-4} .

Finally, we give the expression for the susceptibility χ . Since it is even for Z_m , we only consider the case of $m \geq 0$. In real space, it is given by

$$\begin{aligned} \chi(r, Z_m) &= T \sum_{n=-\infty}^{\infty} G(r, z_n) G(r, z_n + Z_m) \\ &= T \{ 2 \sum_{n=1}^{\infty} G(r, z_n) G(r, z_n + Z_m) \\ &\quad + 2 \sum_{n=1}^{[m/2]} G(r, z_n) G(r, z_n - Z_m) \\ &\quad + G(r, z_{\bar{n}}) G(r, -z_{\bar{n}}) \Big|_{\bar{n}=(m+1)/2} \text{ if } m \text{ is odd} \} \\ &= T \{ 2 \sum_p w_p G(r, z_{n_p}) G(r, z_{n_p} + Z_m) \\ &\quad + 2 \sum_p w_p^{[m/2]} G(r, z_{n_p}) G(r, z_{n_p} - Z_m) \\ &\quad + G(r, z_{\bar{n}}) G(r, -z_{\bar{n}}) \Big|_{\bar{n}=(m+1)/2} \text{ if } m \text{ is odd} \} \\ &\quad + \delta\chi(r, Z_m) \end{aligned}$$

where $[m/2]$ is the integer part of $m/2$, and the last term is given by

$$\delta\chi(r, Z_m) = 2T \sum_{n=N_c+1}^{\infty} G(r, z_n) G(r, z_n + Z_m).$$

Because of $G(r, z_n) \rightarrow \delta_{r0}/z_n$ at $n \rightarrow \infty$, we have

$$\delta\chi(r, Z_m) = \begin{cases} -\frac{\delta_{r0}}{m\pi^2 T} \sum_{n=N_c+1}^{N_c+m} \frac{1}{2n-1}, & \text{if } m > 0 \\ -\frac{2\delta_{r0}}{\pi^2 T} \left[\frac{\pi^2}{8} - \sum_{n=1}^{N_c} \frac{1}{(2n-1)^2} \right], & \text{if } m = 0. \end{cases}$$

Note that $G(r, z_n - Z_m) = G^*(r, Z_m - z_n)$. Therefore, the Green's function at negative Matsubara frequency can be determined from its complex counterpart at the positive frequency. For a given point-selection program, $G(r, z_{np})$ is known. Those values at $Z_m \pm z_n$ can be evaluated by interpolation, or $G(r, z_n + Z_m) \approx \delta_{r0}/(z_n + Z_m)$ if $n + m > N_c$.

APPENDIX B

In this Appendix, we discuss the problem of inverse Fourier transform of $P_{\text{eff}}(\mathbf{q}, 0)$. A typical result for $P_{\text{eff}}(\mathbf{q}, 0)$ is shown in Fig. 7. This function behaves as $P_{\text{eff}}(\mathbf{q}, 0) \propto 1/\sqrt{a^2 + q^2}$ (with $q^2 = q_x^2 + q_y^2$) at $q \rightarrow 0$. The constant a vanishes at $T \leq T_c$. Even at $T > T_c$ but close to T_c , a is very small. Physically, it means that the pairing fluctuation is defined in a long range in real space. Especially, at $T \leq T_c$, the range is infinite. Therefore, its primary form is not suitable for numerical Fourier transform on a finite lattice.

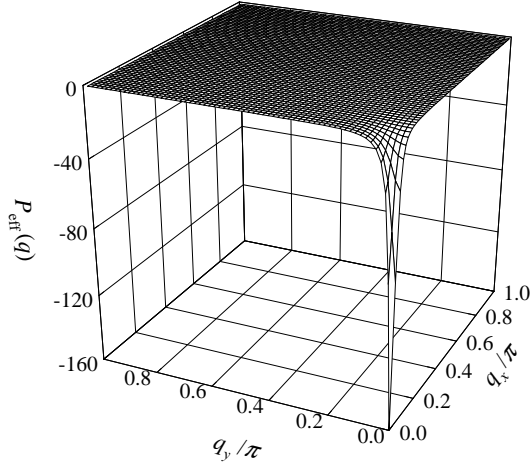


FIG. 7. Function $P_{\text{eff}}(q)$ in unit of $2t$ at $Z_m = 0$, $\delta = 0.125$, and $T/t = 0.0075$.

We divide $P_{\text{eff}}(\mathbf{q}, 0)$ into the ‘singular’ part $c/\sqrt{a^2 + q^2}$ (with c a constant) and the regular one. There is no problem in the Fourier transform for the latter one. For the ‘singular’ part, the task is to calculate the integral

$$F(j_x, j_y) = \int_0^\pi dq_x \int_0^\pi dq_y \frac{\cos(q_x j_x) \cos(q_y j_y)}{\sqrt{a^2 + q^2}}, \quad (\text{B1})$$

where j_x and j_y are the coordinates of a lattice site. Re-

peatedly integrating by part, we get

$$\begin{aligned} F(j_x, j_y) = & -j_y^2 \int_0^\pi dq_x \int_0^\pi dq_y f_1(q) \cos(q_x j_x) \cos(q_y j_y) \\ & + (-1)^{j_y} \int_0^\pi dq_x f_2(q_x) \cos(q_x j_x) \\ & - j_x \int_0^\pi dq_x f_3(q_x) \sin(q_x j_x) \\ & - (-1)^{j_x} f_3(\pi), \end{aligned} \quad (\text{B2})$$

with

$$\begin{aligned} f_1(q) &= q_y \ln(q_y + \sqrt{a^2 + q^2}) - \sqrt{a^2 + q^2} \\ f_2(q_x) &= \ln(\pi + \sqrt{a^2 + \pi^2 + q_x^2}) \\ f_3(q_x) &= q_x (\ln \sqrt{a^2 + q_x^2} - 1) + a \operatorname{atan}\left(\frac{q_x}{a}\right). \end{aligned}$$

By this way, all f 's are regular functions.

However, because the large factors j_y^2 and j_x at long distances, we need to carry out the inverse Fourier transforms in Eq. (B2) with high accuracy. The numerical method of the fast Fourier transforms amounts to applying the trapezoidal rule to the integral in Eq. (B2). One may use a very dense mesh in the Brillouin zone for the transforms. But, this is uneconomical in our numerical process since such transforms need to be repeatedly carried out. In fact, errors in the numerical integration stem mainly from the rapid oscillation behavior in the integrand. Here, we present our scheme for these integrals in Eq. (B2). Essentially, we need to deal with the following integrals,

$$F_c(j) = \int_0^\pi dq f(q) \cos(qj) \quad (\text{B3})$$

$$F_s(j) = \int_0^\pi dq f(q) \sin(qj) \quad (\text{B4})$$

where $f(q)$ is a regular and smooth function over $(0, \pi)$.

Firstly, we consider the simple case,

$$I(q_1, q_3) \equiv \int_{q_1}^{q_3} dq f(q) \cos(qj) \quad (\text{B5})$$

where (q_1, q_3) is a small range. The middle point is q_2 . Within this range, $f(q)$ can be expressed as

$$f(q) \approx a_1 + a_2(q - q_1) + a_3(q - q_1)^2. \quad (\text{B6})$$

The constants a 's are determined by the values $f_j \equiv f(q_j)$,

$$\begin{aligned} a_1 &= f_1 \\ a_2 &= (-3f_1 + 4f_2 - f_3)/2h \\ a_3 &= (f_1 - 2f_2 + f_3)/2h^2, \end{aligned}$$

where $h = q_2 - q_1$. Now, repeatedly integrating Eq. (B5) by part and use Eq. (B6), we obtain

$$I(q_1, q_3) = C_1 \cos(q_1 j) + C_3 \cos(q_3 j) + S_1 \sin(q_1 j) + S_3 \sin(q_3 j) \quad (B7)$$

with

$$\begin{aligned} C_1 &= (3f_1 - 4f_2 + f_3)h/2x^2 \\ C_3 &= (f_1 - 4f_2 + 3f_3)h/2x^2 \\ S_1 &= [f_3 - 2f_2 - (x^2 - 1)f_1]h/x^3 \\ S_3 &= [(x^2 - 1)f_3 + 2f_2 - f_1]h/x^3 \end{aligned}$$

and $x = jh$. It is expectable that the result given by Eq. (B7) is more accurate than the trapezoidal rule.

Now, dividing the range $(0, \pi)$ into $2M$ equal spaced pieces, we have

$$F_c(j) = \sum_{k=1}^M I(q_{2k-1}, q_{2k+1}) \quad (B8)$$

with $q_k = (k-1)h$ and $q_{2M+1} = \pi$. Using the result as given by Eq. (B7), we get

$$\begin{aligned} F_c(j) &= 2w_1(x) \left[2 \sum_{k=2}^M f_{2k-1} \cos(q_{2k-1}j) + f_1 + (-1)^j f_{2M+1} \right] \\ &+ 4w_2(x) \sum_{k=1}^M f_{2k} \cos(q_{2k}j) \end{aligned} \quad (B9)$$

where the functions w_1 and w_2 are given by

$$\begin{aligned} w_1(x) &= \frac{h}{4x^2} \left[3 - \frac{2\sin(2x)}{x} + \cos(2x) \right], \\ w_2(x) &= \frac{h}{x^2} \left(\frac{\sin x}{x} - \cos x \right). \end{aligned}$$

Define a new discrete function

$$g_k = (-1)^k f_k, \quad \text{for } k = 1, \dots, 2M+1.$$

With this definition, equation (B9) can be rewritten as

$$F_c(j) = w_1(x) \{C_j[f] - C_j[g]\} + w_2(x) \{C_j[f] + C_j[g]\} \quad (B10)$$

where $C_j[f]$ is the cosine Fourier transform of function f defined by

$$C_j[f] = 2 \sum_{k=2}^{N-1} f_k \cos(q_k j) + f_1 + (-1)^j f_N$$

with $N = 2M+1$. Therefore, the function $F_c(j)$ can be evaluated by the FFT via Eq. (B10).

Similarly, one can get

$$\begin{aligned} F_s(j) &= w_1(x) \{S_j[f] - S_j[g]\} + w_2(x) \{S_j[f] + S_j[g]\} \\ &+ \frac{h}{x} \left[1 + \frac{\sin(2x)}{2x} - \frac{1 - \cos(2x)}{x^2} \right] [f_1 - (-1)^j f_N] \end{aligned} \quad (B11)$$

where $S_j[f]$ is the sine Fourier transform of function f defined by

$$S_j[f] = 2 \sum_{k=2}^{N-1} f_k \sin(q_k j).$$

APPENDIX C

In this Appendix, we rewrite the eigen equation (6) in a form more convenient for the numerical calculation. This is necessary because the size of the matrix required for Eq. (6) is prohibitive large.

Firstly, we look at the pairing potential. As seen from Figs. 1(c), 1(f) and 3(b), it is given by $V_P(k, k') = V_{1(c)}(k+k') - V_{1(f)}(k-k')$. Since the pairing function $\phi(k)$ can be taken as even function of k , the pairing potential in Eq. (6) can be thereby written as $V_P(k-k')$. The explicit expression is

$$V_P(q) = \frac{3}{2} \frac{U^2 \chi(q)}{1 + U \chi(q)} - \frac{1}{2} \frac{U^2 \chi(q)}{1 - U \chi(q)} - U. \quad (C1)$$

Therefore, the left-hand-side of Eq. (6) is a convolution of V_P and the rest part.

Secondly, we apply the frequency-summation scheme developed in Appendix A to the present case, so reducing the memory size.

However, to solve the eigen equation in momentum space still requires tremendous memory size. Fortunately, we know that the pairing function is short-ranged in real space. We therefore solve the equation in real space. To transform Eq. (6) into real space, one needs to maintain the matrix of the coefficients to be symmetrical. In the follows, we present the transformation procedure.

(A) Define functions $f(\mathbf{k}, n_p)$ and $\psi(\mathbf{k}, n_p)$ as

$$f(\mathbf{k}, n_p) \equiv \sqrt{T w_p G(\mathbf{k}, z_{n_p}) G(-\mathbf{k}, -z_{n_p})}, \quad (C2)$$

$$\psi(\mathbf{k}, n_p) \equiv f(\mathbf{k}, n_p) \phi(\mathbf{k}, z_{n_p}), \quad (C3)$$

where w_p is the weight at frequency z_{n_p} as introduced in Appendix A. In real space, Eq. (6) is transformed to

$$\sum_{\mathbf{r}' p'} A(\mathbf{r}, n_p; \mathbf{r}', n_{p'}) \psi(\mathbf{r}', n_{p'}) = \lambda \psi(\mathbf{r}, n_p) \quad (C4)$$

with

$$A(\mathbf{r}, n_p; \mathbf{r}', n_{p'}) = \sum_{\mathbf{R}} f(\mathbf{r} - \mathbf{R}, n_p) W(\mathbf{R}, n_p, n_{p'}) f(\mathbf{R} - \mathbf{r}', n_{p'}) \quad (C5)$$

and

$$W(\mathbf{R}, n_p, n_{p'}) = V_P(\mathbf{R}, z_{n_p} - z_{n_{p'}}) + V_P(\mathbf{R}, z_{n_p} + z_{n_{p'}}). \quad (C6)$$

(B) Further more, because of the lattice symmetry, we need only to consider the lattice sites $[r]$ of $0 \leq r_y < r_x$.

Those lattice sites of $r_x = r_y$ are excluded since the d -wave pairing is under consideration. Define

$$y(\mathbf{r}, n) = 2\sqrt{\frac{2}{d_r}}\psi(\mathbf{r}, n) \quad (C7)$$

$$F(\mathbf{r}, \mathbf{R}, n) = \frac{1}{\sqrt{d_r d_R}} \sum_g s_g f(g\mathbf{r} - \mathbf{R}, n) \quad (C8)$$

where $d_r = 1 + \delta_{r_y 0}$, the g -summation runs over the operations of group C_{4v} , $s_g = \pm 1$ is the sign factor of the d -wave function $\phi(\mathbf{r}, z_n)$ under the operation g , and $g\mathbf{r}$ denotes a site coming from \mathbf{r} operated by g . Accordingly, define the new matrix

$$M(\mathbf{r}, n_p; \mathbf{r}', n_{p'}) = \sum_{[\mathbf{R}]} F(\mathbf{r}, \mathbf{R}, n_p) W(\mathbf{R}, n_p, n_{p'}) F(\mathbf{r}', \mathbf{R}, n_{p'}) \quad (C9)$$

where again $[\mathbf{R}]$ -summation runs over those lattice sites of $0 \leq R_y < R_x$. By so doing, the eigen equation reads,

$$\sum_{[\mathbf{r}']_{p'}} M(\mathbf{r}, n_p; \mathbf{r}', n_{p'}) y(\mathbf{r}', n_{p'}) = \lambda y(\mathbf{r}, n_p). \quad (C10)$$

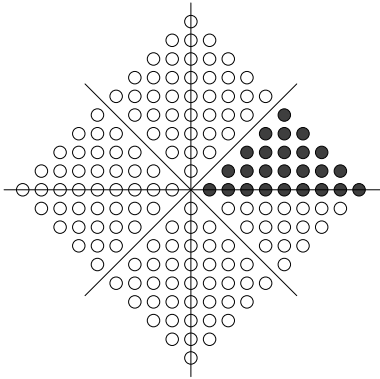


FIG. 8. Lattice sites used for solving Eq. (C10).

In our numerical calculation, the region $[r]$ is taken as the shaded sites as shown in Fig. 8, which is suitable for the description of d -wave pairing. The total number of sites of $[r]$ is $N_r = 25$. The normalization condition for $y(\mathbf{r}, n_p)$ is

$$\sum_{[\mathbf{r}]_p} y^2(\mathbf{r}, n_p) = 1. \quad (C11)$$

By this condition, the coupling constant v is given as $v = \lambda/2$. Shown in Fig. 9 are the typical results for $f(r_x, 1)$ and $\phi(r_x, z_1)$. Clearly, they are short-ranged functions. This fact justifies that the size of $[r]$ is reasonable. In passing, we compare the sizes of matrices of coefficients required for solving the eigen equation respectively in real and momentum spaces. The dimension of matrix M in Eq. (C9) is $(N_r M_0) \times (N_r M_0) = 1425 \times 1425$, where

$M_0 = 57$ is the number of selected Matsubara frequency. However, in momentum space with a 128×128 mesh, even making use of the lattice symmetry, the dimension is $(N_k M_0) \times (N_k M_0) = 118560 \times 118560$, where $N_k = 32 \times 65$ is the number of momentum \mathbf{k} with $0 \leq k_y < k_x \leq \pi$.

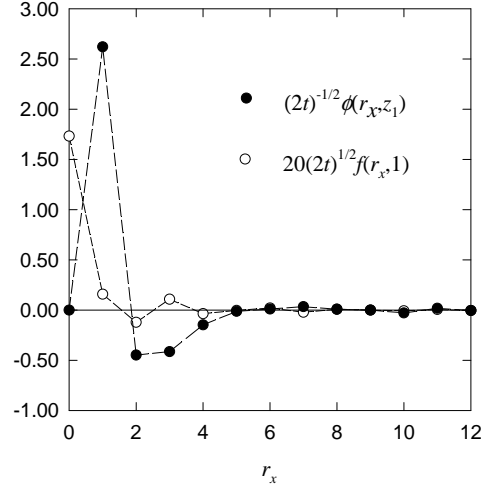


FIG. 9. Functions $f(r_x, 1)$ and $\phi(r_x, z_1)$ at $r_y = 0$, $\delta = 0.125$, and $T_c/t = 0.0075$. The dashed lines are for the eyes.

-
- ¹ P. W. Anderson, *Science* **235**, 1196 (1987).
 - ² Z. Y. Weng, T. K. Lee, and C. S. Ting, *Phys. Rev. B* **38**, 6561 (1988).
 - ³ J. R. Schrieffer, X. G. Wen, and S. C. Zhang, *Phys. Rev. Lett.* **60**, 944 (1988); *Phys. Rev. B* **39**, 11663 (1989).
 - ⁴ G. Vignale and K. S. Singwei, *Phys. Rev. B* **39**, 2956 (1989).
 - ⁵ N. E. Bickers, D. J. Scalapino and S. R. White, *Phys. Rev. Lett.* **62**, 961 (1989).
 - ⁶ P. Monthoux and D. J. Scalapino, *Phys. Rev. Lett.* **72**, 1874 (1994).
 - ⁷ C. H. Pao and N. E. Bickers, *Phys. Rev. Lett.* **72**, 1870 (1994); *Phys. Rev. B* **49**, 1586 (1994); *ibid.* **51**, 16310 (1995).
 - ⁸ T. Dahm and T. Tewordt, *Phys. Rev. B* **52**, 1297 (1995).
 - ⁹ R. Putz, R. Preuss, A. Muramatsu, and W. Hanke, *Phys. Rev. B* **53**, 5133 (1996).
 - ¹⁰ S. Koikegami, S. Fujimoto, and K. Yamada, *J. Phys. Soc. Jpn.* **66**, 1438 (1997).
 - ¹¹ T. Takimoto and T. Moriya, *J. Phys. Soc. Jpn.* **66**, 2459 (1997); **67**, 3570 (1998).
 - ¹² H. Kontani, K. Kanki, and K. Ueda, *Phys. Rev. B* **59**, 14723 (1999).
 - ¹³ V. J. Emery and S. A. Kivelson, *Nature* **374**, 434 (1995);

- E. Babaev and H. Kleinert, Phys. Rev. B **59**, 12083 (1999).
- ¹⁴ For a recent review, see, V. M. Loktev, R. M. Quick, and S. G. Sharapov, Phys. Rep., **349**, 1 (2001).
- ¹⁵ B. Jankó, J. Maly, and K. Levin, Phys. Rev. B **56**, 11407 (1997); I. Kosztin, Q. J. Chen, Y. J. Kao, and K. Levin, Phys. Rev. B **61**, 11662 (2000); Q. Chen, I. Kosztin, B. Jankó, and K. Levin, Phys. Rev. Lett. **81**, 4708 (1998); Phys. Rev. Lett. **85**, 2801 (2001).
- ¹⁶ X. Z. Yan, Int. J. Mod. Phys. B **17**, 319 (2003); J. Phys. Condens. Matter **15**, L319 (2003).
- ¹⁷ N. D. Mermin and H. Wagner, Phys. Rev. Lett. **17**, 1133 (1966); P. C. Hohenberg, Phys. Rev. **158**, 383 (1967).
- ¹⁸ C. A. R. Sá de Melo, M. Randeria, and J. R. Engelbrecht, Phys. Rev. Lett. **71**, 3202 (1993); Phys. Rev. B **55**, 15153 (1997).
- ¹⁹ J. R. Engelbrecht, A. Nazarenko, M. Randeria, and E. Dagotto, Phys. Rev. B. **57**, 13406 (1998); T. Hotta, M. Mayr, and E. Dagotto, *ibid.* **60**, 13085 (1999).
- ²⁰ B. Kyung, S. Allen, and A. -M. S. Tremblay, Phys. Rev. B **64**, 075 116 (2001).
- ²¹ H. Kontani, Phys. Rev. Lett. **89**, 237003 (2002).
- ²² G. V. M. Williams, J. L. Tallon, R. Michalak, and R. Dupree, Phys. Rev. B **54**, 6909 (1996).
- ²³ Ch. Renner, B. Revaz, J. -Y. Genoud, K. Kadowaki, and Ø. Fischer, Phys. Rev. Lett. **80**, 149 (1998); V. M. Krasnov, A. Yurgens, D. Winkler, P. Delsing, and T. Claeson, Phys. Rev. Lett. **84**, 5860 (2000); M. Suzuki and T. Watanabe, Phys. Rev. Lett. **85**, 4787 (2000).
- ²⁴ J. L. Tallon, J. W. Loram, J. R. Cooper, C. Panagopoulos, and C. Bernhard, Phys. Rev. B **68**, 180501 (2003).
- ²⁵ J. Hubbard, Proc. Roy. Soc., Ser. A **276**, 238 (1963); *ibid.* **277**, 237 (1963).
- ²⁶ J. L. Tallon, C. Bernhard, H. Shaked, R. L. Hitterman, and J. D. Jorgensen, Phys. Rev. B **51**, 12911 (1995), and references therein.
- ²⁷ J. J. Deisz, D. W. Hess, and J. W. Serene, Phys. Rev. Lett. **76**, 1312 (1996).

TABLE I. Ratio of Sum given by Eq. (A11) and $S_n = 2n/(2n + 1)$ at varies n . $R.E.$ represents the relative error.

n	Sum/S_n	$R.E.$
5.	1.000000	0
10.	1.000047	0.000047
50.	1.000012	0.000012
100.	1.000013	0.000013
500.	1.000013	0.000013